Volcanic Cloud Evolution: Characteristics, Observational Capabilities and Challenges

David J. Schneider[1], Michael Pavolonis[2], Simon Carn[3]

[1] U.S. Geological Survey, Alaska Volcano Observatory, 4230 University Drive, Anchorage, Alaska 99508
[2] NOAA Cooperative Institute for Meteorological Satellite Studies, University of Wisconsin – Madison, 1225 W. Dayton St., Room 207, Madison, WI 53706
[3] Michigan Technological University, Geological and Mining Engineering and Sciences, 1400 Townsend Drive, Houghton, MI 4993
UNITED STATES OF AMERICA

djschneider@usgs.gov

ABSTRACT

Volcanic clouds composed of solid particles, volcanic gases, and related aerosols evolve from the time of eruption until the cloud constituents are removed from the atmosphere. While airborne, they have the potential to cause damage to aircraft, ranging from acute encounters that can lead to an immediate hazard to flight safety, to chronic wear on aircraft components, to benign encounters where no observable impacts occur. We highlight the evolution of cloud properties through three stages: Stage 1 (recent), through Stage 2 (intermediate), to Stage 3 (final) and comment on the current observational capabilities and challenges of detection and characterization of volcanic clouds.

1.0 INTRODUCTION

Volcanic clouds produced by explosive eruptions are well known to present acute and chronic hazards to aviation, resulting in disruptions to flight operations, safety of flight concerns, and increased frequency of maintenance procedures [1-3]. Volcanic clouds are composed of a mixture of solid particles (rock, glass, and mineral fragments), volcanic gases (water, sulfur dioxide, hydrogen sulfide, carbon dioxide, and hydrogen halides) and a variety of aerosols that form from the gaseous components. The volcano explosivity index (VEI) is used to characterize the relative magnitude of eruptions based primarily on the volume of erupted products and the maximum volcanic cloud height [4]. While imperfect, it does provide a method to compare eruptions. Eruptions of greatest concern to aircraft at cruise altitude typically fall in the range of VEI 3 to VEI 6, with eruption volumes of 0.01 to 10 km^3 (on a logarithmic scale) and cloud altitudes of 3 to >25 km. The global frequency of eruption is inversely proportional to eruption size, with a VEI 3 eruption occurring every few months, VEI 4 every year, VEI 5 every 10 years and VEI 6 every 100 years (Table 1).

Table 1: Volcanic Explosivity Index (VEI) and related parameters.

VEI	Cloud Height (km)	Eruption Volume (m^3)	Duration (hours)	Tropospheric Injection	Stratospheric Injection	Frequency
0	< 0.1 m	< $1x10^4$	< 1	Negligible	None	Constant
1	0.1 to 10	> $1x10^4$	< 1	Minor	None	Daily
2	1 to 5	> $1x10^6$	1 to 6	Moderate	None	Weekly
3	3 to 15	> $1x10^7$	1 to 12	Substantial	Possible	Yearly
4	10 to 25	> $1x10^8$	1 to >12	Substantial	Definite	≥ 10 years
5	> 25	> $1x10^9$	6 to > 12	Substantial	Significant	≥ 50 years
6	> 25	> $1x10^{10}$	> 12	Substantial	Significant	≥ 100 years
7	> 25	> $1x10^{11}$	> 12	Substantial	Significant	≥ 1000 years
8	> 25	> $1x10^{12}$	> 12	Substantial	Significant	≥ 10,000 years

2.0 VOLCANIC CLOUD EVOLUTION

Volcanic clouds show variation in erupted magma composition (as measured by silica content), particle size distribution (a function of the fragmentation process), and the amount of volcanic gas released with the solid ash particles. These properties evolve over time as the cloud disperses in the atmosphere, which changes the hazards, as well as the methods used to detect and track them. We propose that three stages in cloud evolution can be used to describe some of these changes.

Stage 1 volcanic clouds pertain to the first several hours of residence time in the atmosphere (Fig. 1A). During this stage, eruption column processes are active (formation of ice particles and aggregate growth) [5-7] and volcanic material can be distributed many kilometers vertically. The majority of ash particles with diameters less than about 0.5 mm sediment out of the cloud during this time period. Eruptions that produce clouds large enough to pose a hazard to aircraft at cruise altitude are typically visible in meteorological satellite data, provided they are not obscured or mixed with significant meteorological clouds (Fig. 1B). They contain particles large enough to be observed on ground-based meteorological radar and can rise to aircraft cruise altitude (>9 km) within minutes of eruption onset (Fig. 1C) [8]. Many of the most serious aircraft encounters that have caused acute aircraft damage resulting in engine shutdown have occurred in the first several hours of volcanic cloud residence times within several hundred kilometers of the eruption site. [1]

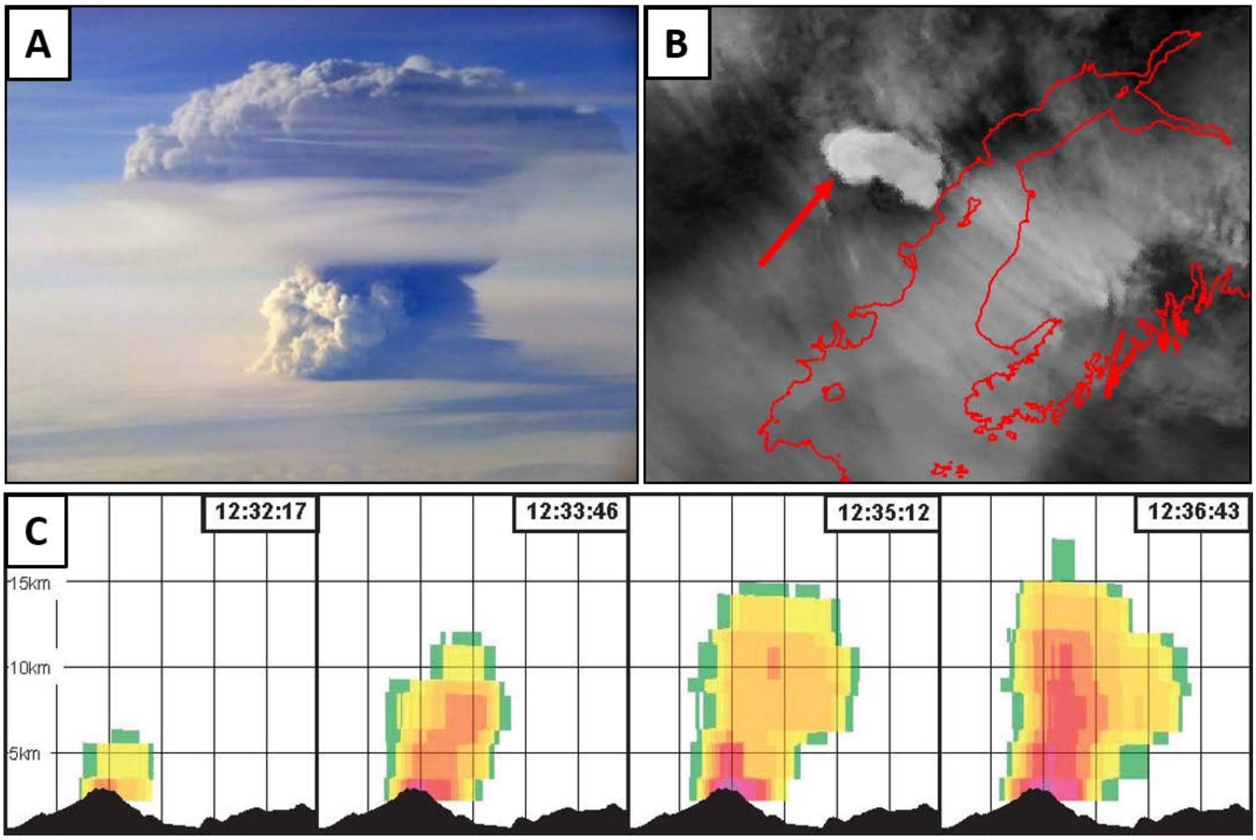

Figure 1: Stage 1 volcanic clouds from Redoubt Volcano, Alaska in 2009 (A) Photograph of the volcanic eruption taken from an aircraft at an altitude of ~35,000 ft asl on March 28, 2009 at 01:45 UTC. (B) Thermal infrared satellite image of a Stage 1 volcanic cloud (red arrow) collected on March 24, 2009 at 04:30 UTC. In this image the temperature scale ranges from black (warm) to white (cold). (C) Sequence of radar cross sections through a Stage 1 volcanic cloud collected on March 23, 2009. Start time of radar scan (~90 second duration) indicated in UTC. Radar reflectivity ranges from 20 to 60 dBZ (green to purple).

Stage 2 volcanic clouds are those with residence times in the atmosphere of several hours to several days after eruption. During this stage there is the potential for acute (safety of flight), chronic (increased wear), or non-damaging aircraft encounters. [1,9]. Volcanic cloud expansion by wind advection and diffusion shears the cloud into layers several km thick vertically. Particle aggregation and fallout of very-fine to fine-grained ash occurs, and in many cases the volcanic ash and sulfur dioxide constituents of the cloud are able to be observed using thermal infrared [10] and ultraviolet remote sensing methods [11] (Fig. 2). The volcanic ash “signal” (e.g., thermal infrared brightness temperature difference) decreases more rapidly than the sulfur dioxide “signal” in days following the eruption. The volcanic ash and sulfur dioxide clouds typically follow similar trajectories as the cloud disperses, as seen in the example from Kasatochi shown in Fig. 2. However, in other cases there is a vertical separation of volcanic ash and gas, which in the presence of wind shear will transport the cloud constituents in different directions [12-13].

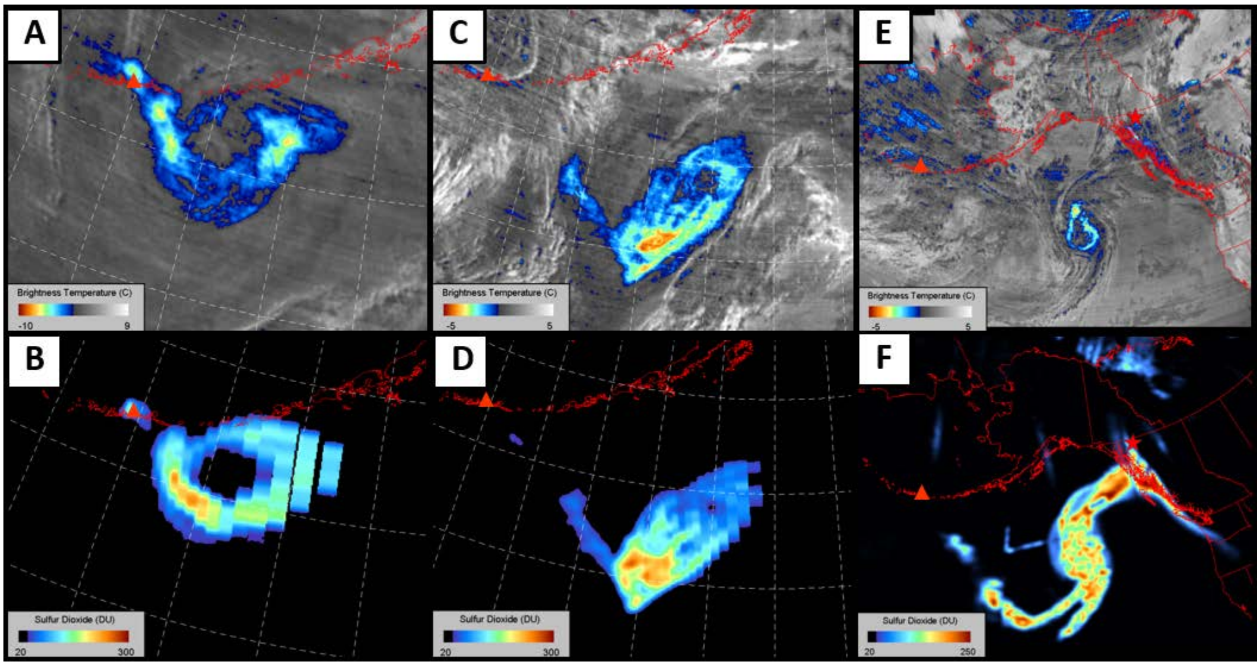

Figure 2: Stage 2 volcanic ash (A, C, and E) and sulfur dioxide (B, D, and F) clouds from the 2008 eruption of Kasatochi Volcano, Alaska. The location of the volcano is shown by the red triangle. The cloud location is shown at 20 hours (A-B), 40 hours (C-D) and, 66 hours (E-F) after eruption onset. The volcanic ash extent as detected by the GOES imager is depicted as the thermal infrared brightness temperature difference. Note that the magnitude of the signal does not scale linearly with the mass of airborne ash. The sulphur dioxide cloud as detected by the OMI sensor is depicted in Dobson Units, which is the retrieved total column abundance of the UV absorbing gas. The location of a non-damaging aircraft encounter over western Canada is shown as a red star in Fig. 2 E-F and described in Guffanti et al. [9]

Stage 3 volcanic clouds are observed in the days to weeks following an eruption, until the cloud is no longer detectable using remote sensing methods. These drifting volcanic clouds may be transported thousands of kilometers from the volcano (Fig. 3A), and in some cases circumnavigate the earth. They are typically present as very thin layers less than a kilometer thick (Fig. 3B, Fig. 4C) and can be cause for concern for pilots [14]. Very-fine-grained ash (micron size) may be present in these clouds, but at very low total column mass values that are below the detection limit of current thermal-infrared satellite techniques (less than 0.01 to 0.1 g/m^2) [15-16]. These clouds are observed using visible [17], ultraviolet [18], and thermal infrared [19] remote sensing techniques that can detect sulfate aerosol (Fig. 4A) and sulfur dioxide [20] (Fig. 4B). Acute damage to aircraft from these clouds is unlikely but there is the potential for chronic aircraft damage over time.

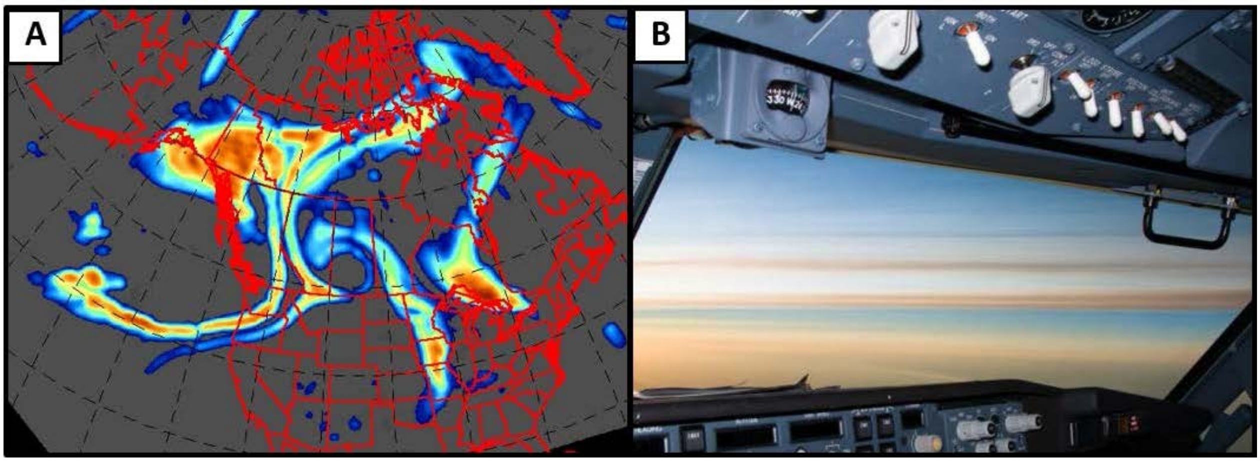

Figure 3: Stage 3 volcanic clouds. (A) Sulfur dioxide cloud from Kasatochi Volcano, Alaska one week after the end of eruptive activity as detected by the OMI sensor. (B) Volcanic aerosol layers (presumably sulfate from the conversion of sulfur dioxide) from the 2008 eruption of Okmok Volcano, Alaska as seen from an aircraft flying at 28,000 ft over Billings, Montana one week after the end of eruptive activity. (Image courtesy of Bradley Johnson and Alaska Airlines)

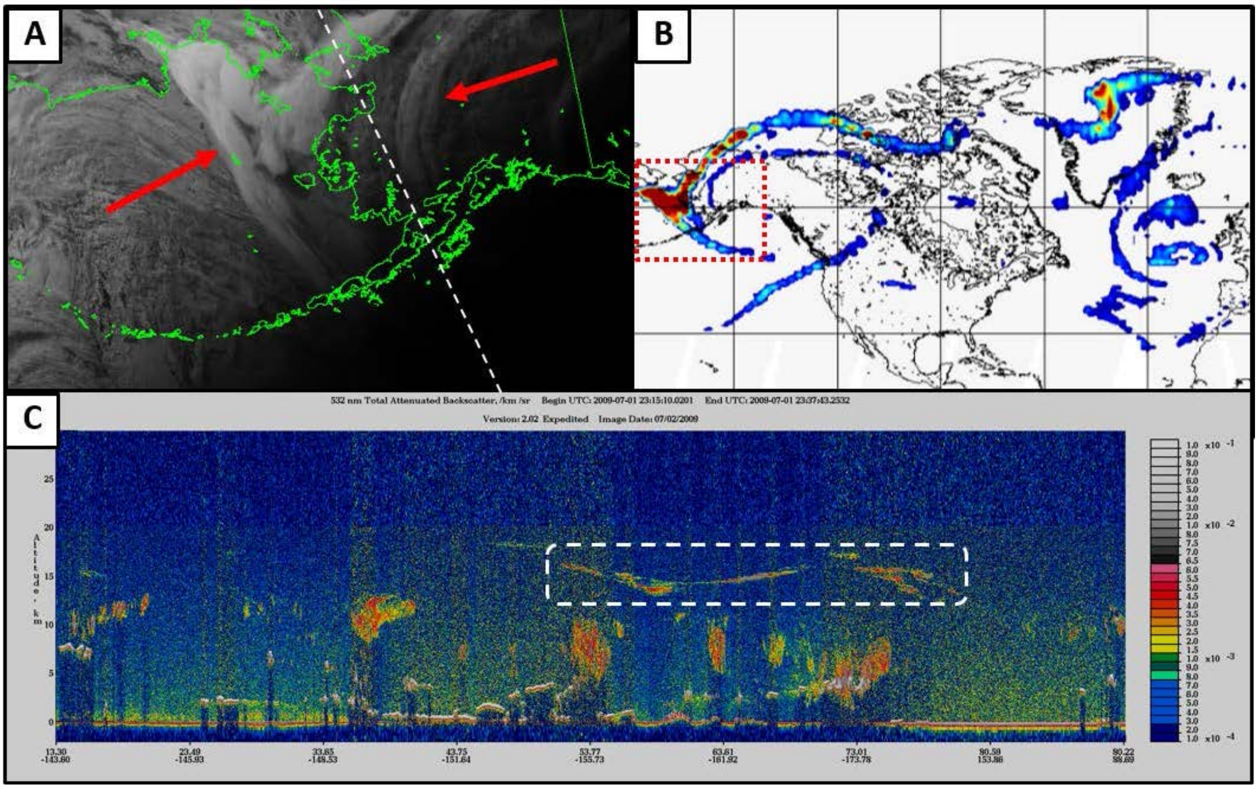

Figure 4: Stage 3 volcanic clouds from the 2009 eruption of Sarychev Peak, Russia approximately two weeks after the end of eruptive activity. A) GOES visible satellite image showing a high altitude volcanic cloud (red arrows) above the meteorological cloud deck. This cloud was only visible during sunset as forward scatter enhanced the volcanic aerosol cloud. The location of the lidar cross section shown in Fig. 4C is indicated by the dashed white line. B) Extent of the sulfur dioxide cloud as detected by the IASI sensor. Image produced by Université Libre de Bruxelles. The red box indicates the approximate extent of the GOES image shown in Fig. 4A. C) CALIOP satellite lidar total attenuated cross-section of meteorological and volcanic cloud layers. The white dashed box indicates the vertical and along-track extent of the Sarychev Peak aerosol layer.

3.0 OBSERVATIONAL CAPABILITIES

Explosive volcanic eruptions and their resultant clouds can be observed and characterized by various geophysical and satellite methods. The primary geophysical methods used by volcano observatories include seismic (used for forecasting, detecting and characterizing eruptions) [21-23], infrasound (detection and characterization of volcanic explosions) [24-26], web cameras (eruption cloud height) [27-28], lightning sensors (detecting ash emissions) [26, 29-31] and radar (cloud height, structure, grain size characteristics) [8, 32-34]. These capabilities vary widely between countries and between different regions within countries.

Once a volcano erupts, satellite methods are used by (some) volcano observatories and by the nine regional Volcanic Ash Advisory Centers (VAAC) to detect and confirm ash emissions, characterize volcanic cloud height (for input into ash transport and dispersion models), and to evaluate the accuracy of the forecast regions of ash hazard [35]. Automated, objective image processing techniques have been developed to detect volcanic ash clouds, identify cloud objects and retrieve cloud parameters from satellite data [36-40] (Fig. 5). The VOLcanic Cloud Analysis Toolkit (VOLCAT) operates globally to produce global alerts of volcanic activity for use by volcano observatories and the VAACs (https://volcano.ssec.wisc.edu/). High-temporal resolution geostationary satellite data now available from Himawari-8 (Japan), GOES-R (United States) and Seviri (European Union) allow for automated detection of energetic explosive eruptions on the basis of their anomalously high growth rate (compared to normal convective cloud formation) [41]. Global web-based images products of sulfur dioxide and volcanic ash is available from the Support to Aviation Control Service (SACS) project, which uses data derived from UV/Visible and Infrared sensors on board of several polar-orbiting satellites (http://sacs.aeronomie.be/index.php).

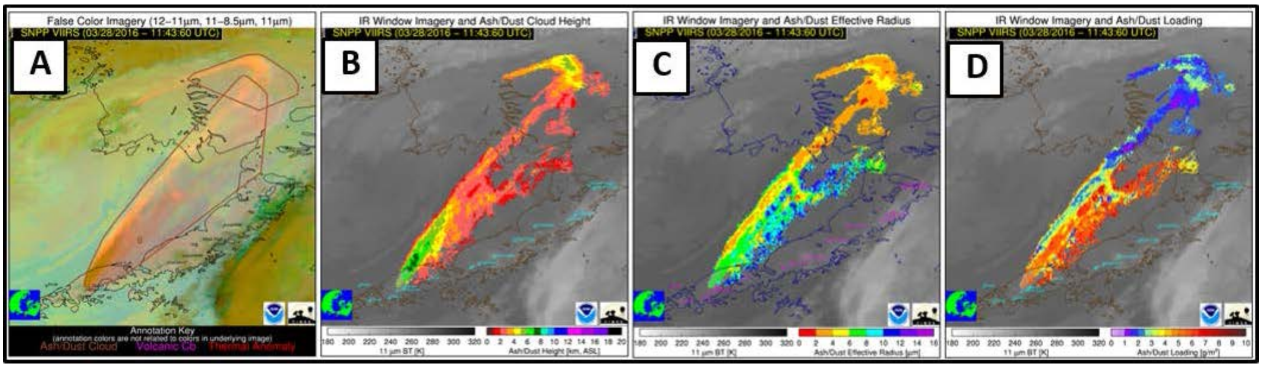

Figure 5: (A) Multispectral false-color composite and retrieved parameters of (B) ash cloud height, (C) ash particle effective radius, and (D) volcanic ash mass loading from a VIIRS satellite image of the volcanic cloud from Pavlof Volcano collected on 28 March 2016.

4.0 OBSERVATIONAL CHALLANGES

Although significant capabilities exist, challenges remain. Seismic and infrasound monitoring are effective means to detect explosive eruptions, but it is not possible at the onset of eruption to determine whether significant ash emission is occurring, the total mass that will be erupted, and how long the eruption will continue. In particular, it is difficult to characterize the key eruption source parameters, such as mass eruption rate, in real-time. Particle size and vertical mass distribution are also critical for initializing ash transport and dispersion models, but not easily determined during an eruption. Characterization by satellite methods can be hampered by environmental factors such as complexity in the local meteorological clouds, layers in the volcanic clouds, particle size and compositional complexity, and by limited regional satellite observing capabilities. New satellite data sources have increased temporal, spatial, and spectral resolution, with more planned for the future. The developments call for automated techniques to identify regions and time periods of potential volcanic ash hazards for evaluation by skilled analysts. Satellite and geophysical monitoring data sources exist that can improve operational response and hazard notification, but they are currently widely dispersed at various space and meteorological agencies, as well as volcano observatories. Aviation user needs to address chronic exposure concerns require information on ash concentration observations and forecasts. Continued evaluation of the capabilities of satellite retrievals schemes and dispersion model output is required.

5.0 REFERENCES

[1] Guffanti, M., Casadevall, T. J., & Budding, K. (2010). *Encounters of aircraft with volcanic ash clouds; a compilation of known incidents, 1953-2009*, [Online] http://pubs.usgs.gov/ds/545/. U.S. Geological Survey Data Series 545.

[2] Casadevall, T. J. (1994). The 1989–1990 eruption of Redoubt Volcano, Alaska: impacts on aircraft operations. *Journal of Volcanology and Geothermal Research*, *62*(1-4), 301-316.

[3] Casadevall, T. J., Delos Reyes, P. J., & Schneider, D. J. (1996). The 1991 Pinatubo eruptions and their effects on aircraft operations. *Fire and Mud: eruptions and lahars of Mount Pinatubo, Philippines*, 625-636.

[4] Newhall, C. G., & Self, S. (1982). The volcanic explosivity index (VEI) an estimate of explosive magnitude for historical volcanism. *Journal of Geophysical Research: Oceans*, *87*(C2), 1231-1238.

[5] Brown, R. J., Bonadonna, C., & Durant, A. J. (2012). A review of volcanic ash aggregation. *Physics and Chemistry of the Earth, Parts A/B/C*, *45*, 65-78.

[6] Durant, A.J. and R.J. Brown, (2016), "Chapter 2 – Ash Aggregation in Volcanic Clouds", In *Volcanic Ash*, ed. by Shona Mackie, Katharine Cashman, Hugo Ricketts, Alison Rust and Matt Watson, Elsevier, 2016, 53-65, ISBN 9780081004050. DOI: 10.1016/B978-0-08-100405-0.00006-9

[7] Van Eaton, A. R., Mastin, L. G., Herzog, M., Schwaiger, H. F., Schneider, D. J., Wallace, K. L., & Clarke, A. B. (2015). Hail formation triggers rapid ash aggregation in volcanic plumes. *Nature Communications*, *6*, 7860.

[8] Schneider, D. J., & Hoblitt, R. P. (2013). Doppler weather radar observations of the 2009 eruption of Redoubt Volcano, Alaska. *Journal of Volcanology and Geothermal Research*, *259*, 133-144.

[9] Guffanti, M., Schneider, D. J., Wallace, K. L., Hall, T., Bensimon, D. R., & Salinas, L. J. (2010). Aviation response to a widely dispersed volcanic ash and gas cloud from the August 2008 eruption of Kasatochi, Alaska, USA. *Journal of Geophysical Research: Atmospheres*, *115*(D2).

[10] Prata, A. J. (1989). Observations of volcanic ash clouds in the 10-12 μm window using AVHRR/2 data. *International journal of Remote sensing*, *10*(4-5), 751-761.

[11] Carn, S. A., Krueger, A. J., Krotkov, N. A., Yang, K., & Evans, K. (2009). Tracking volcanic sulfur dioxide clouds for aviation hazard mitigation. *Natural Hazards*, *51*(2), 325-343.

[12] Schneider, D. J., Rose, W. I., Coke, L. R., Bluth, G. J., Sprod, I. E., & Krueger, A. J. (1999). Early evolution of a stratospheric volcanic eruption cloud as observed with TOMS and AVHRR. *Journal of Geophysical Research: Atmospheres*, *104*(D4), 4037-4050.

[13] Moxnes, E. D., Kristiansen, N. I., Stohl, A., Clarisse, L., Durant, A., Weber, K., & Vogel, A. (2014). Separation of ash and sulfur dioxide during the 2011 Grímsvötn eruption. *Journal of Geophysical Research: Atmospheres*, *119*(12), 7477-7501.

[14] Weinzierl, B., Sauer, D., Minikin, A., Reitebuch, O., Dahlkötter, F., Mayer, B., ... & Veira, A. (2012). On the visibility of airborne volcanic ash and mineral dust from the pilot's perspective in flight. *Physics and Chemistry of the Earth, Parts A/B/C*, *45*, 87-102.

[15] Prata, A. J., & Prata, A. T. (2012). Eyjafjallajökull volcanic ash concentrations determined using Spin Enhanced Visible and Infrared Imager measurements. *Journal of Geophysical Research: Atmospheres*, *117*(D20).

[16] WMO SCOPE-Nowcasting. Meeting on the Intercomparison of Satellite-based Volcanic Ash Retrieval Algorithms Final Report. [Online] 2015. http://www.wmo.int/pages/prog/sat/documents/SCOPE-NWC-PP2_VAIntercompWSReport2015.pdf

[17] Winker, D. M., Vaughan, M. A., Omar, A., Hu, Y., Powell, K. A., Liu, Z., ... & Young, S. A. (2009). Overview of the CALIPSO mission and CALIOP data processing algorithms. *Journal of Atmospheric and Oceanic Technology*, *26*(11), 2310-2323.

[18] Carn, S. A., Krotkov, N. A., Yang, K., Hoff, R. M., Prata, A. J., Krueger, A. J., ... & Levelt, P. F. (2007). Extended observations of volcanic SO 2 and sulfate aerosol in the stratosphere. *Atmospheric Chemistry and Physics Discussions*, *7*(1), 2857-2871.

[19] Karagulian, F., Clarisse, L., Clerbaux, C., Prata, A. J., Hurtmans, D., & Coheur, P. F. (2010). Detection of volcanic SO2, ash, and H2SO4 using the Infrared Atmospheric Sounding Interferometer (IASI). *Journal of Geophysical Research: Atmospheres*, *115*(D2).

[20] Carn, S. A., Clarisse, L., & Prata, A. J. (2016). Multi-decadal satellite measurements of global volcanic degassing. *Journal of Volcanology and Geothermal Research*, *311*, 99-134.

[21] Chouet, B. A., & Matoza, R. S. (2013). A multi-decadal view of seismic methods for detecting precursors of magma movement and eruption. *Journal of Volcanology and Geothermal Research*, *252*, 108-175.

[22] White, Randall, and Wendy McCausland. "Volcano-tectonic earthquakes: A new tool for estimating intrusive volumes and forecasting eruptions." *Journal of Volcanology and Geothermal Research* 309 (2016): 139-155.

[23] Prejean, S. G., & Brodsky, E. E. (2011). Volcanic plume height measured by seismic waves based on a mechanical model. *Journal of Geophysical Research: Solid Earth*, *116*(B1).

[24] Fee, D., & Matoza, R. S. (2013). An overview of volcano infrasound: From Hawaiian to Plinian, local to global. *Journal of Volcanology and Geothermal Research*, *249*, 123-139.

[25] Matoza, R. S., Le Pichon, A., Vergoz, J., Herry, P., Lalande, J. M., Lee, H. I., ... & Rybin, A. (2011). Infrasonic observations of the June 2009 Sarychev Peak eruption, Kuril Islands: Implications for infrasonic monitoring of remote explosive volcanism. *Journal of Volcanology and Geothermal Research*, *200*(1), 35-48.

[26] Fee, D., Haney, M. M., Matoza, R. S., Eaton, A. R., Cervelli, P., Schneider, D. J., & Iezzi, A. M. (2017). Volcanic tremor and plume height hysteresis from Pavlof Volcano, Alaska. *Science*, *355*(6320), 45-48.

[27] Corradini, S., Montopoli, M., Guerrieri, L., Ricci, M., Scollo, S., Merucci, L., ... & Grainger, R. G. (2016). A multi-sensor approach for volcanic ash cloud retrieval and eruption characterization: The 23 November 2013 Etna lava fountain. *Remote Sensing*, *8*(1), 58.

[28] Vulpiani, G., Ripepe, M., & Valade, S. (2016). Mass discharge rate retrieval combining weather radar and thermal camera observations. *Journal of Geophysical Research: Solid Earth*, *121*(8), 5679-5695.

[29] Hoblitt, R. P. (1994). An experiment to detect and locate lightning associated with eruptions of Redoubt Volcano. *Journal of Volcanology and Geothermal research*, *62*(1-4), 499-517.

[30] Thomas, R. J., McNutt, S. R., Krehbiel, P. R., Rison, W., Aulich, G., Edens, H. E., and Clark, E., Lightning and electrical activity during the 2006 eruption of Augustine Volcano, in J. Powers, M. Coombs, J. Freymueller (Eds.), The 2006 Eruption of Augustine Volcano, Alaska. U.S. Geological Survey Professional Paper 1769 (2010), pp. 579–608

[31] Behnke, S. A., Thomas, R. J., McNutt, S. R., Schneider, D. J., Krehbiel, P. R., Rison, W., & Edens, H. E. (2013). Observations of volcanic lightning during the 2009 eruption of Redoubt Volcano. *Journal of Volcanology and Geothermal Research*, *259*, 214-234.

[32] Marzano, F. S., Barbieri, S., Vulpiani, G., & Rose, W. I. (2006). Volcanic ash cloud retrieval by ground-based microwave weather radar. *IEEE Transactions on Geoscience and Remote Sensing*, *44*(11), 3235-3246.

[33] Arason, P., Petersen, G. N., & Bjornsson, H. (2011). Observations of the altitude of the volcanic plume during the eruption of Eyjafjallajökull, April–May 2010. *Earth System Science Data*, *3*(1), 9-17.

[34] Marzano, F. S., Picciotti, E., Montopoli, M., & Vulpiani, G. (2013). Inside volcanic clouds: Remote sensing of ash plumes using microwave weather radars. *Bulletin of the American Meteorological Society*, *94*(10), 1567-1586.

[35] Bonadonna, C., Folch, A., Loughlin, S., & Puempel, H. (2012). Future developments in modelling and monitoring of volcanic ash clouds: outcomes from the first IAVCEI-WMO workshop on Ash Dispersal Forecast and Civil Aviation. *Bulletin of volcanology*, *74*(1), 1-10.

[36] Pavolonis, M.J., W.F. Feltz, A.K. Heidinger, and G.M. Gallina, “A daytime complement to the reverse absorption technique for improved automated detection of volcanic ash,” *Journal of Atmospheric and Oceanic Technology*, 23, 1422-1444, 2006.

[37] Pavolonis, M.J., “Advances in Extracting Cloud Composition Information from Spaceborne Infrared Radiances-A Robust Alternative to Brightness Temperatures. Part I: Theory,” *Journal of Applied Meteorology and Climatology,* 49, doi:10.1175/2010JAMC2433.1, 2010.

[38] Pavolonis, M., A.K. Heidinger, and J. Sieglaff, “Automated retrievals of volcanic ash and dust cloud properties from upwelling infrared measurements,” *Journal Geophysical Research-Atmospheres*, 118, doi:10.1002/jgrd.50173, 2013.

[39] Pavolonis, M., J. Sieglaff, and J. Cintineo), “Spectrally Enhanced Cloud Objects (SECO): A Generalized Framework for Automated Detection of Volcanic Ash and Dust Clouds using Passive Satellite

Measurements, Part I: Multispectral Analysis," *Journal Geophysical Research-Atmospheres*, 120(15), 7813-7841. 2015.

[40] Pavolonis, M., J. Sieglaff, and J. Cintineo, "Spectrally Enhanced Cloud Objects (SECO): A Generalized Framework for Automated Detection of Volcanic Ash and Dust Clouds using Passive Satellite Measurements, Part II: Cloud Object Analysis and Global Application," *Journal Geophysical Research-Atmospheres*, 120(15), 7842-7870, 2015.

[41] Pavolonis, M.J., J. Cintineo, and J. Sieglaff, "Automated Detection of Explosive Volcanic Eruptions Using Satellite-derived Cloud Vertical Growth Rates," *Journal Geophysical Research*, in prep.